Electronic Supplementary Material (ESI) for Physical Chemistry Chemical Physics.

Supplemental Material

to

Hindered Rotor Benchmarks for the Transition States of Free Radical Additions to Unsaturated Hydrocarbons

Yanjin Sun, [1]* Kieran P. Somers, [1] Quan-De Wang, [1, 2] Caoimhe Farrell, [1] Henry J. Curran[1]*

[1] Combustion Chemistry Centre, School of Chemistry, Ryan Institute, MaREI, National University of Ireland, Galway, Ireland

[2] Low Carbon Energy Institute and School of Chemical Engineering, Jiangsu Province Engineering Laboratory of High Efficient Energy Storage Technology and Equipment, China University of Mining and Technology, Xuzhou, 221008, People's Republic of China

* Corresponding author: y.sun5@nuigalway.ie,

henry.curran@nuigalway.ie

1. The bond lengths of the newly formed rotors for the TSs of $\dot{C}H_3$, $\dot{C}_2H_3$, $\dot{C}_2H_5$, $CH_3\dot{O}$ radical additions to C_2H_2, which are calculated at CCSD(T)-F12/cc-pVDZ-F12 and twelve DFT methods.

Table S1 The bond lengths of the newly formed rotors for the TSs of $\dot{C}H_3$, $\dot{C}_2H_3$, $\dot{C}_2H_5$, $CH_3\dot{O}$ radical additions to C_2H_2.

Label	**Ṙ**	**CCSD(T)-F12**	**B2PLYP-D3**			**B3LYP**			**M06-2X**			**ωB97X-D**		
		cc-pVDZ-F12	**6-31+G(d,p)**	**6-311++G(d,p)**	**cc-pVTZ**	**6-31+G(d,p)**	**6-311++G(d,p)**	**cc-pVTZ**	**6-31+G(d,p)**	**6-311++G(d,p)**	**cc-pVTZ**	**6-31+G(d,p)**	**6-311++G(d,p)**	**cc-pVTZ**
TS1	**$\dot{C}H_3$**	2.24	2.26	2.23	2.23	2.34	2.30	2.30	2.24	2.22	2.22	2.29	2.26	2.26
TS9	**$\dot{C}_2H_3$**	2.28	2.30	2.27	2.27	2.40	2.33	2.34	2.28	2.26	2.25	2.32	2.29	2.29
TS17	**$\dot{C}_2H_5$**	2.24	2.25	2.23	2.23	2.33	2.29	2.29	2.23	2.21	2.21	2.28	2.25	2.25
TS25	**$CH_3\dot{O}$**	1.98	1.98	1.96	1.97	2.02	1.99	2.00	1.97	1.95	1.96	2.00	1.97	1.98

2. The dihedrals of the newly formed rotors for the TSs of $\dot{C}H_3$, $\dot{C}_2H_3$, $\dot{C}_2H_5$, $CH_3\dot{O}$ radical additions to C_2H_2, which are calculated at CCSD(T)-F12/cc-pVDZ-F12 and twelve DFT methods.

Table S2 The dihedrals of the newly formed rotors for the TSs of $\dot{C}H_3$, $\dot{C}_2H_3$, $\dot{C}_2H_5$, $CH_3\dot{O}$ radical additions to C_2H_2.

Label	**Ṙ**	**CCSD(T)-F12**	**B2PLYP-D3**			**B3LYP**			**M06-2X**			**ωB97X-D**		
		cc-pVDZ-F12	**6-31+G(d,p)**	**6-311++G(d,p)**	**cc-pVTZ**	**6-31+G(d,p)**	**6-311++G(d,p)**	**cc-pVTZ**	**6-31+G(d,p)**	**6-311++G(d,p)**	**cc-pVTZ**	**6-31+G(d,p)**	**6-311++G(d,p)**	**cc-pVTZ**
TS1	**$\dot{C}H_3$**	–0.96	0.00	0.00	0.00	0.00	0.00	0.00	0.00	0.00	0.00	0.00	0.00	0.00
TS9	**$\dot{C}_2H_3$**	47.07	64.60	64.68	53.44	–180.00	80.03	72.09	47.30	–169.83	–42.00	60.33	59.35	54.98
TS17	**$\dot{C}_2H_5$**	0.86	0.00	0.00	0.00	0.00	0.00	0.00	0.00	0.00	0.00	0.00	0.00	0.00
TS25	**$CH_3\dot{O}$**	1.94	0.00	0.00	0.00	0.00	0.00	0.00	0.00	0.00	0.00	0.00	0.00	0.00

3. The T1 diagnostic values of the CCSD(T)/cc-pVQZ calculations for the TSs of $\dot{C}H_3$, $\dot{C}_2H_3$, $\dot{C}_2H_5$, $CH_3\dot{O}$ radical additions to C_2H_2 and C_2H_4.

Table S3 T1 diagnostic values of the CCSD(T)/cc-pVQZ calculations

Reactant		T1 diagnostic
A	B	CCSD(T)/cc-pVQZ
C_2H_2	$\dot{C}H_3$	0.0383
C_2H_4		0.0302
C_2H_2	$\dot{C}_2H_3$	0.0446
C_2H_4		0.0398
C_2H_2	$\dot{C}_2H_5$	0.0336
C_2H_4		0.0271
C_2H_2	$CH_3\dot{O}$	0.0344
C_2H_4		0.0311

4. **Table S4** The maximum differences of the hindered barriers calculated by twelve DFT methods for the newly formed internal rotors in target reactions. (kJ mol^{-1})

Label	Reac. *B*	ΔE_{HR}^{max}	Label	Reac. *B*	ΔE_{HR}^{max}
$\dot{C}H_3$ addition					
TS1	C_2H_2	0.30	TS2	C_2H_4	0.79
TS3	C_3H_4-a(E)	0.53	TS4	C_3H_4-a(I)	0.49
TS5	C_3H_4-p(E)	0.39	TS6	C_3H_4-p(I)	0.67
TS7	C_3H_6(E)	0.84	TS8	C_3H_6(I)	1.30
$\dot{C}_2H_3$ addition					
TS9	C_2H_2	1.10	TS10	C_2H_4	1.91
TS11	C_3H_4-a(E)	2.21	TS12	C_3H_4-a(I)	2.30
TS13	C_3H_4-p(E)	1.55	TS14	C_3H_4-p(I)	1.24
TS15	C_3H_6(E)	2.65	TS16	C_3H_6(I)	2.01
$\dot{C}_2H_5$ addition					
TS17	C_2H_2	2.42	TS18	C_2H_4	2.36
TS19	C_3H_4-a(E)	1.98	TS20	C_3H_4-a(I)	1.41
TS21	C_3H_4-p(E)	3.02	TS22	C_3H_4-p(I)	3.16
TS23	C_3H_6(E)	2.71	TS24	C_3H_6(I)	2.31
$CH_3\dot{O}$ addition					
TS25	C_2H_2	4.40	TS26	C_2H_4	2.38
TS27	C_3H_4-a(E)	3.56	TS28	C_3H_4-a(I)	5.78
TS29	C_3H_4-p(E)	6.73	TS30	C_3H_4-p(I)	4.62
TS31	C_3H_6(E)	4.39	TS32	C_3H_6(I)	3.43

5. **Table S5** The maximum differences of rotational constants calculated by twelve DFT methods for the newly formed internal rotors in target reactions. (cm^{-1})

Label	Reac. B	$\Delta B(\chi)_{max}$	Label	Reac. B	$\Delta B(\chi)_{max}$
$\dot{C}H_3$ addition					
TS1	C_2H_2	0.13	TS2	C_2H_4	0.09
TS3	C_3H_4-a(E)	0.12	TS4	C_3H_4-a(I)	0.07
TS5	C_3H_4-p(E)	0.14	TS6	C_3H_4-p(I)	0.08
TS7	C_3H_6(E)	0.13	TS8	C_3H_6(I)	0.08
$\dot{C}_2H_3$ addition					
TS9	C_2H_2	0.18	TS10	C_2H_4	0.09
TS11	C_3H_4-a(E)	0.12	TS12	C_3H_4-a(I)	0.13
TS13	C_3H_4-p(E)	0.14	TS14	C_3H_4-p(I)	0.10
TS15	C_3H_6(E)	0.20	TS16	C_3H_6(I)	0.11
$\dot{C}_2H_5$ addition					
TS17	C_2H_2	0.14	TS18	C_2H_4	0.06
TS19	C_3H_4-a(E)	0.09	TS20	C_3H_4-a(I)	0.05
TS21	C_3H_4-p(E)	0.04	TS22	C_3H_4-p(I)	0.04
TS23	C_3H_6(E)	0.13	TS24	C_3H_6(I)	0.04
$CH_3\dot{O}$ addition					
TS25	C_2H_2	0.15	TS26	C_2H_4	0.19
TS27	C_3H_4-a(E)	0.17	TS28	C_3H_4-a(I)	0.30
TS29	C_3H_4-p(E)	0.08	TS30	C_3H_4-p(I)	0.07
TS31	C_3H_6(E)	0.25	TS32	C_3H_6(I)	0.11

6. **Table S6** The maximum percentage errors of Q_{HR} as a function of temperature calculated by twelve DFT methods for the newly formed internal rotors in target reactions. (in percentage)

Label	Reac. *B*	$\frac{Q_{HR}^{DFT_{max}} - Q_{HR}^{DFT_{min}}}{Q_{HR}^{DFT_{min}}}$	Label	Reac. *B*	$\frac{Q_{HR}^{DFT_{max}} - Q_{HR}^{DFT_{min}}}{Q_{HR}^{DFT_{min}}}$
$\dot{C}H_3$ addition					
TS1	C_2H_2	2.81	TS2	C_2H_4	8.43
TS3	C_3H_4-a(E)	5.49	TS4	C_3H_4-a(I)	6.05
TS5	C_3H_4-p(E)	4.11	TS6	C_3H_4-p(I)	7.32
TS7	C_3H_6(E)	9.31	TS8	C_3H_6(I)	12.64
$\dot{C}_2H_3$ addition					
TS9	C_2H_2	15.79	TS10	C_2H_4	62.43
TS11	C_3H_4-a(E)	51.75	TS12	C_3H_4-a(I)	32.78
TS13	C_3H_4-p(E)	17.04	TS14	C_3H_4-p(I)	22.68
TS15	C_3H_6(E)	87.08	TS16	C_3H_6(I)	49.61
$\dot{C}_2H_5$ addition					
TS17	C_2H_2	77.85	TS18	C_2H_4	31.44
TS19	C_3H_4-a(E)	20.27	TS20	C_3H_4-a(I)	37.56
TS21	C_3H_4-p(E)	123.54	TS22	C_3H_4-p(I)	49.74
TS23	C_3H_6(E)	21.81	TS24	C_3H_6(I)	16.84
$CH_3\dot{O}$ addition					
TS25	C_2H_2	30.4	TS26	C_2H_4	9.16
TS27	C_3H_4-a(E)	11.06	TS28	C_3H_4-a(I)	17.55
TS29	C_3H_4-p(E)	77.30	TS30	C_3H_4-p(I)	42.83
TS31	C_3H_6(E)	41.33	TS32	C_3H_6(I)	35.47

7. Rotational constants for the newly formed rotors of $\dot{C}H_3/\dot{C}_2H_3/\dot{C}_2H_5/CH_3\dot{O}$ radical additions to $C_2H_2/C_2H_4/C_3H_4$-a/C_3H_4-p/C_3H_6 calculated at twelve DFT methods.

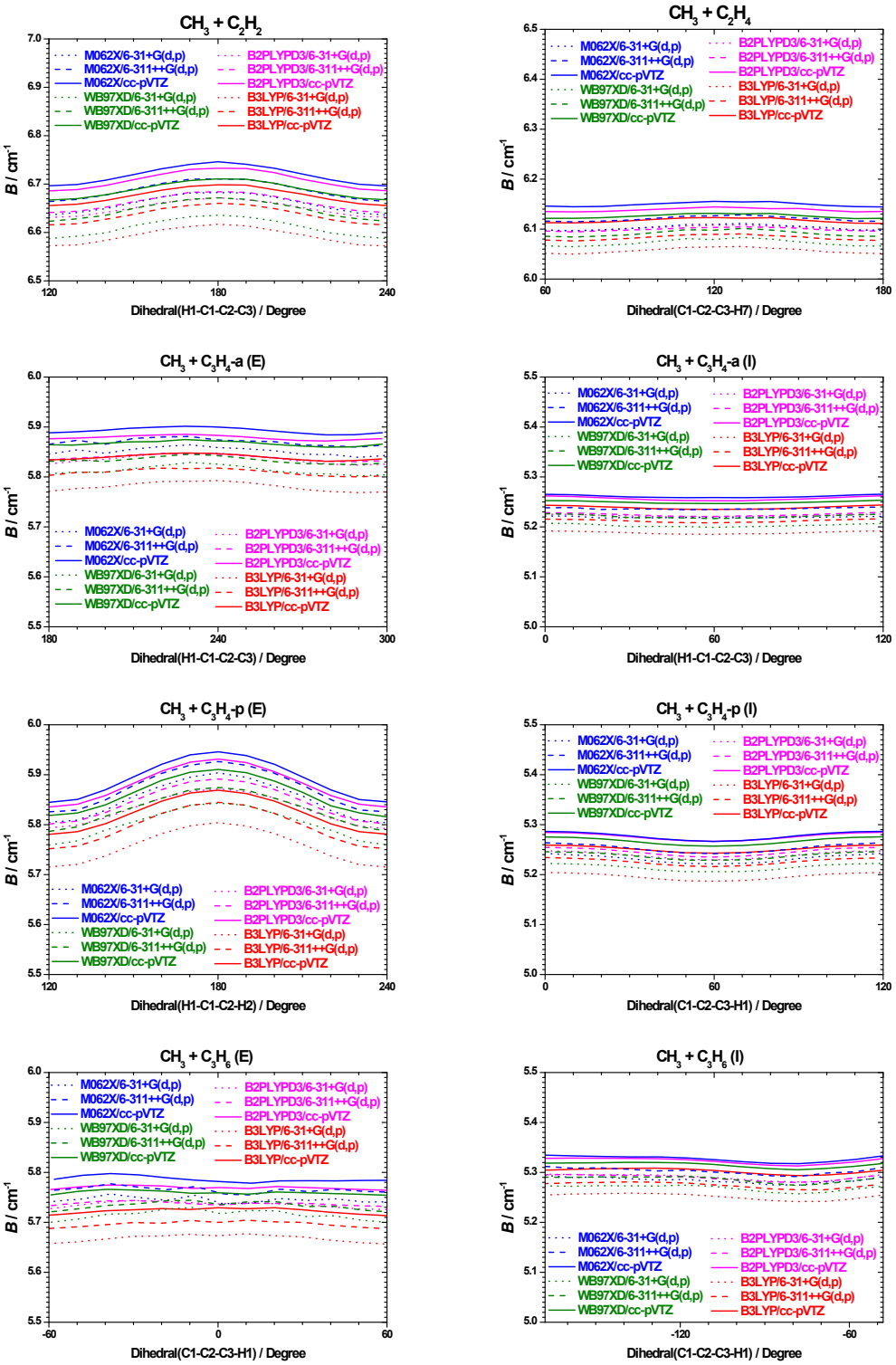

Fig. S1 Rotational constants for the newly formed methyl rotors of $\dot{C}H_3$ radical additions to $C_2H_2/C_2H_4/C_3H_4$-a/C_3H_4-p/C_3H_6 calculated at twelve DFT methods.

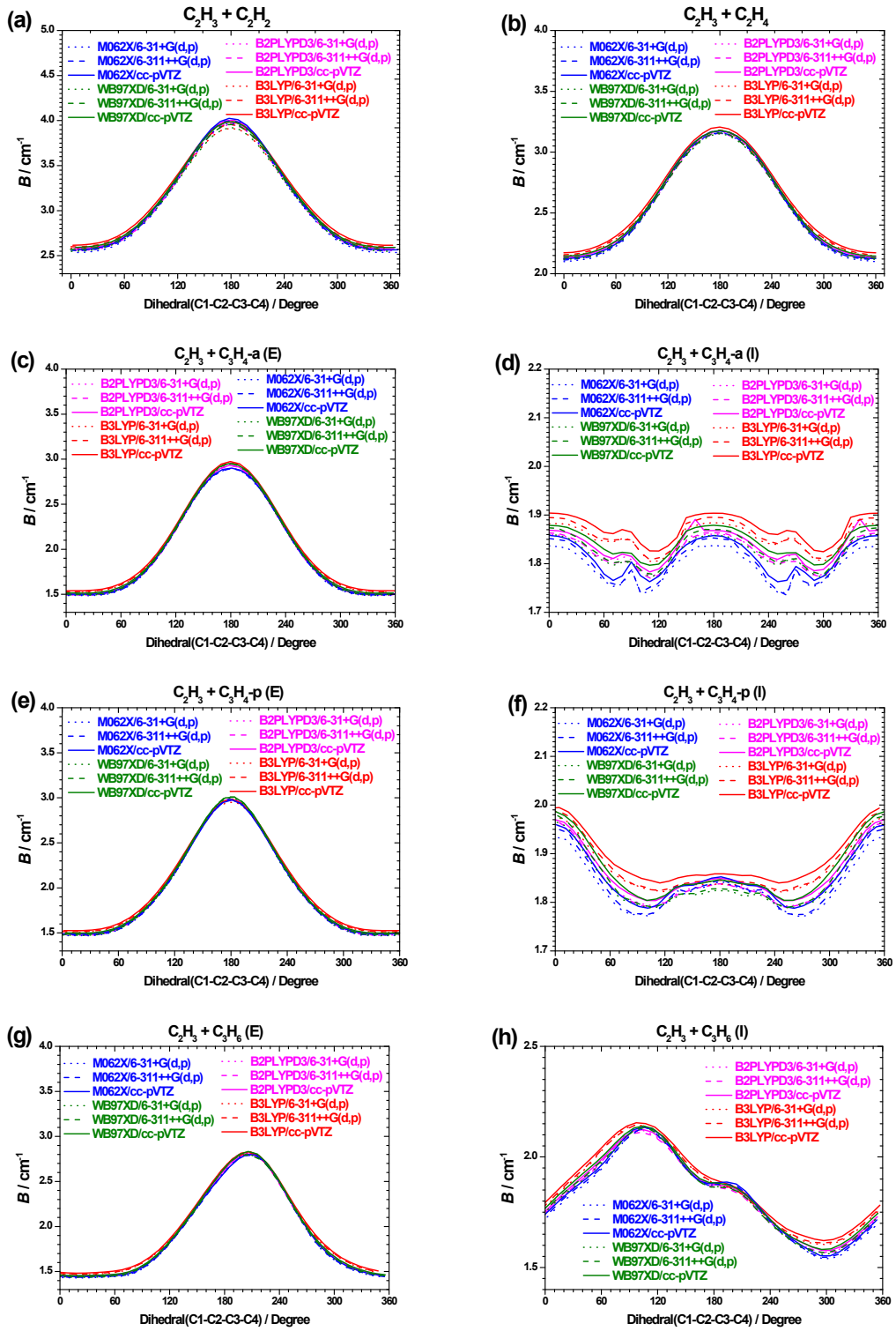

Fig. S2 Rotational constants for rotors formed by $\dot{C}_2H_3$ radical additions to C_2H_2/C_2H_4/C_3H_4-a/C_3H_4-p/C_3H_6 calculated at twelve DFT methods.

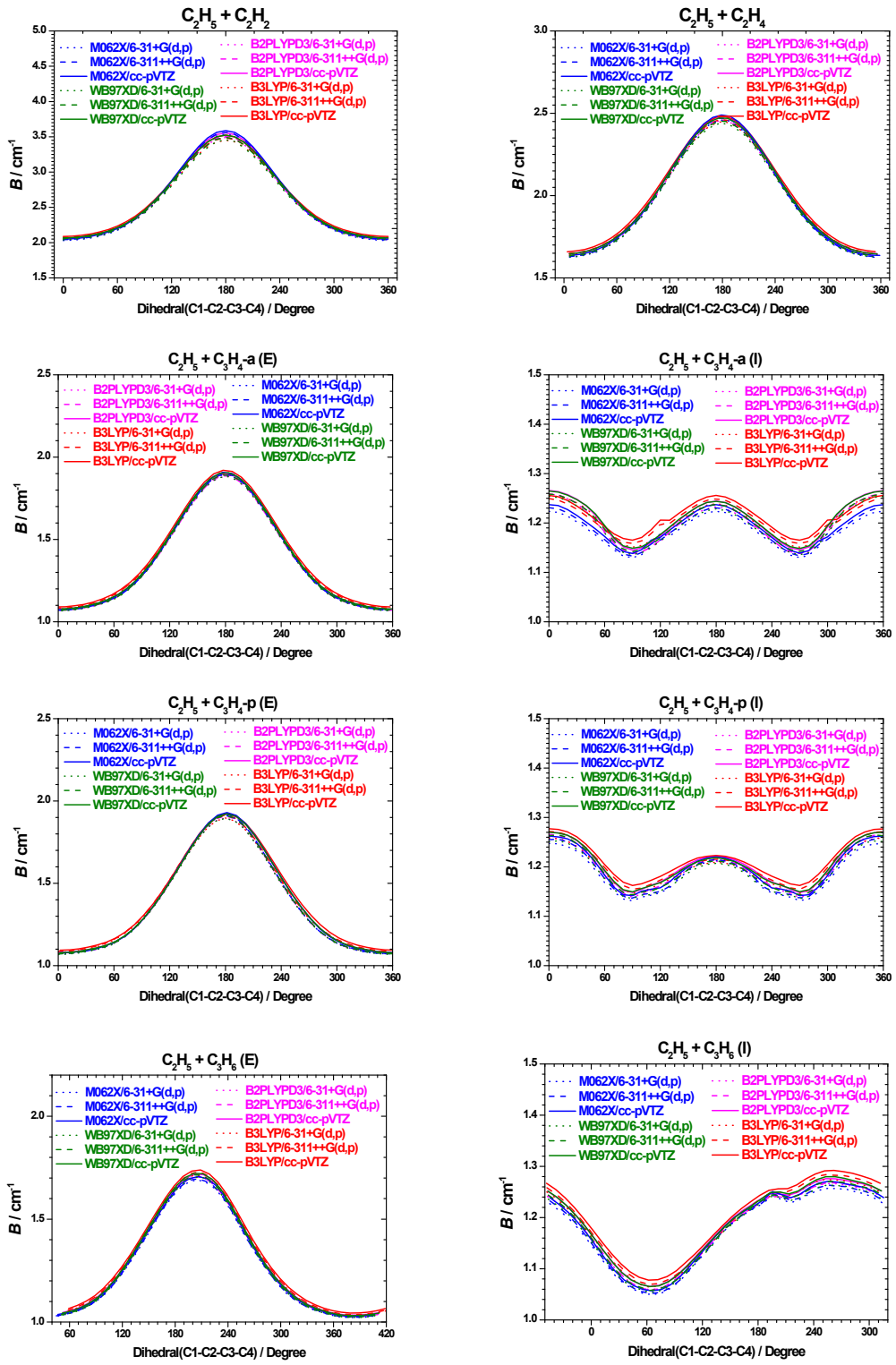

Fig. S3 Rotational constants for rotors formed by $\dot{C}_2H_5$ radical additions to C_2H_2/C_2H_4/C_3H_4-a/C_3H_4-p/C_3H_6 calculated at twelve DFT methods.

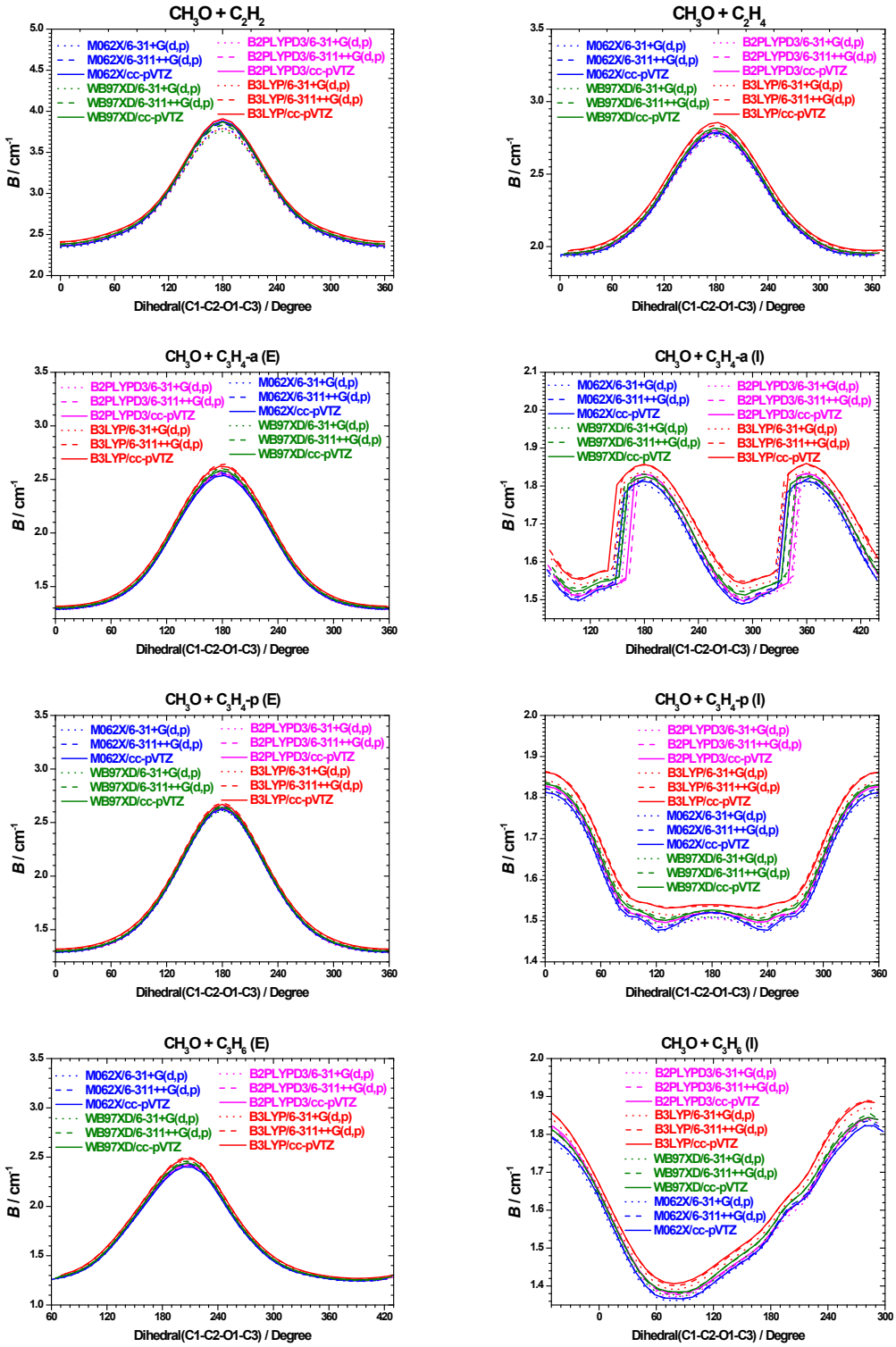

Fig. S4 Rotational constants for rotors formed by $CH_3\dot{O}$ radical additions to C_2H_2/C_2H_4/C_3H_4-a/C_3H_4-p/C_3H_6 calculated at twelve DFT methods.

8. Hindrance potentials for the newly formed rotors of $\dot{C}H_3/\dot{C}_2H_3/\dot{C}_2H_5/CH_3\dot{O}$ radical additions to $C_2H_2/C_2H_4/C_3H_4$-a/C_3H_4-p/C_3H_6 calculated at twelve DFT methods.

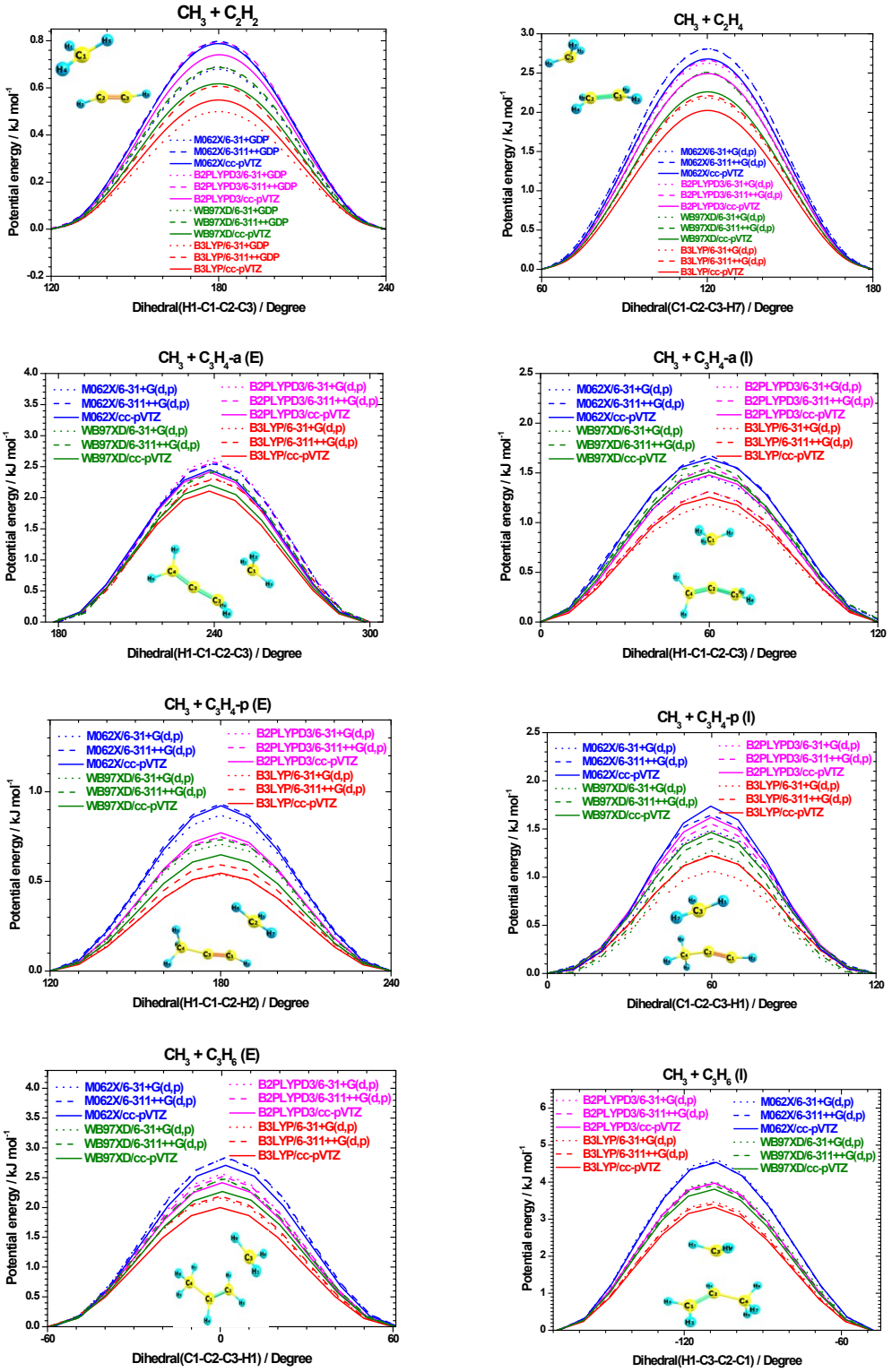

Fig. S5 Hindrance potentials for the newly formed methyl rotors of $\dot{C}H_3$ radical additions to $C_2H_2/C_2H_4/C_3H_4$-a/C_3H_4-p/C_3H_6 calculated at twelve DFT methods.

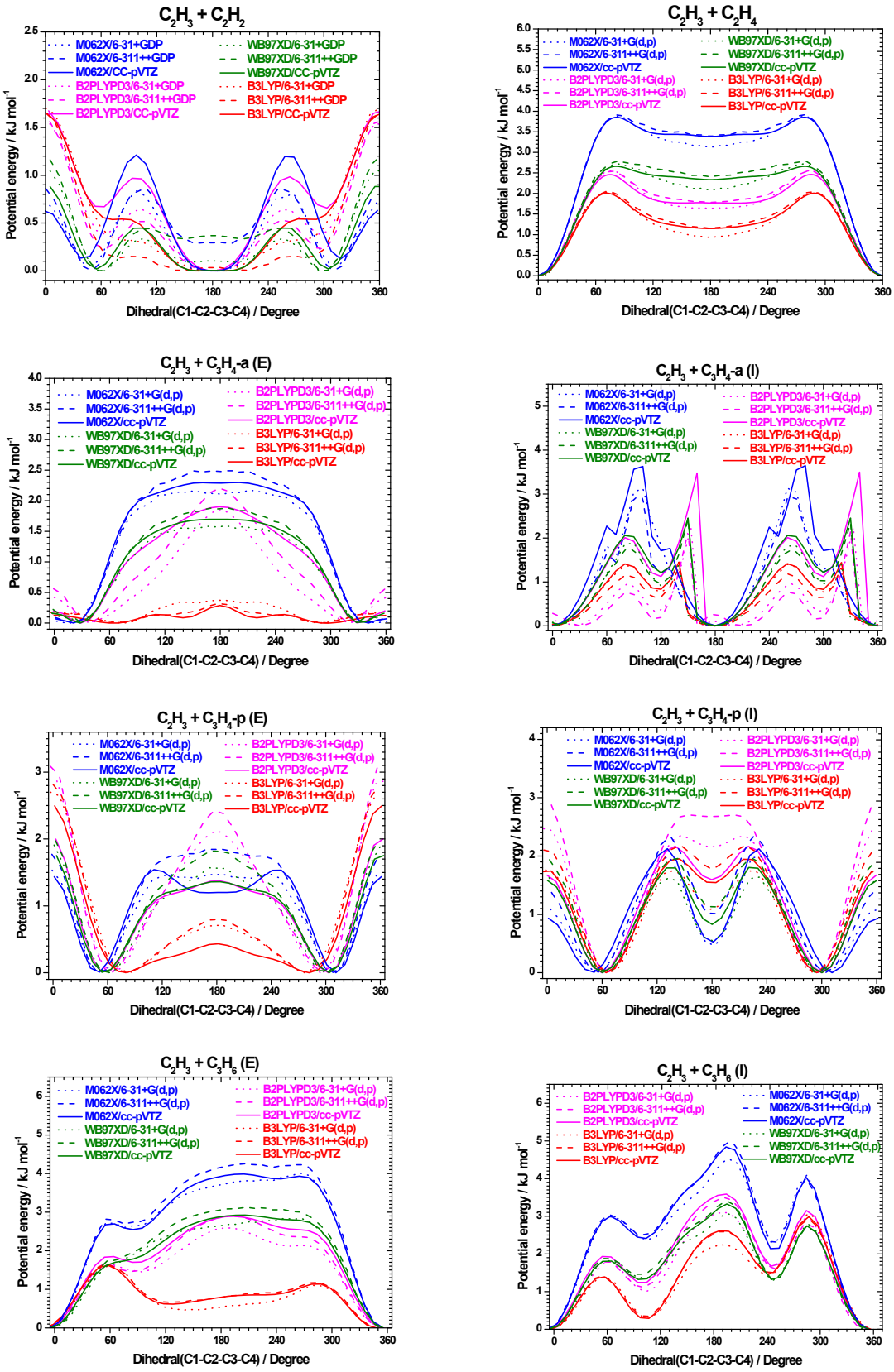

Fig. S6 Hindrance potentials for the newly formed methyl rotors of $\dot{C}_2H_3$ radical additions to C_2H_2/C_2H_4/C_3H_4-a/C_3H_4-p/C_3H_6 calculated at twelve DFT methods.

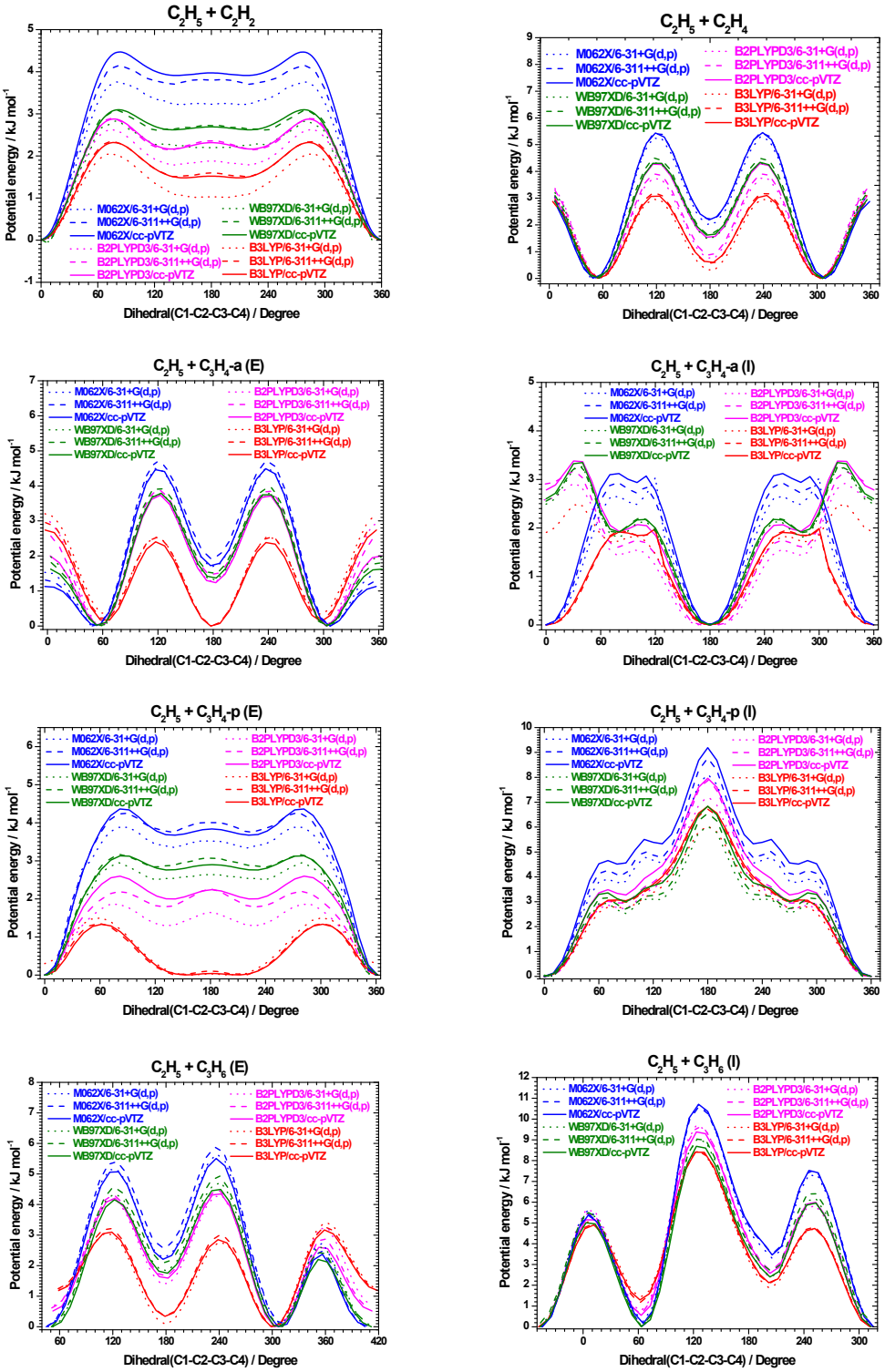

Fig. S7 Hindrance potentials for the newly formed methyl rotors of $\dot{C}_2H_5$ radical additions to C_2H_2/C_2H_4/C_3H_4-a/C_3H_4-p/C_3H_6 calculated at twelve DFT methods.

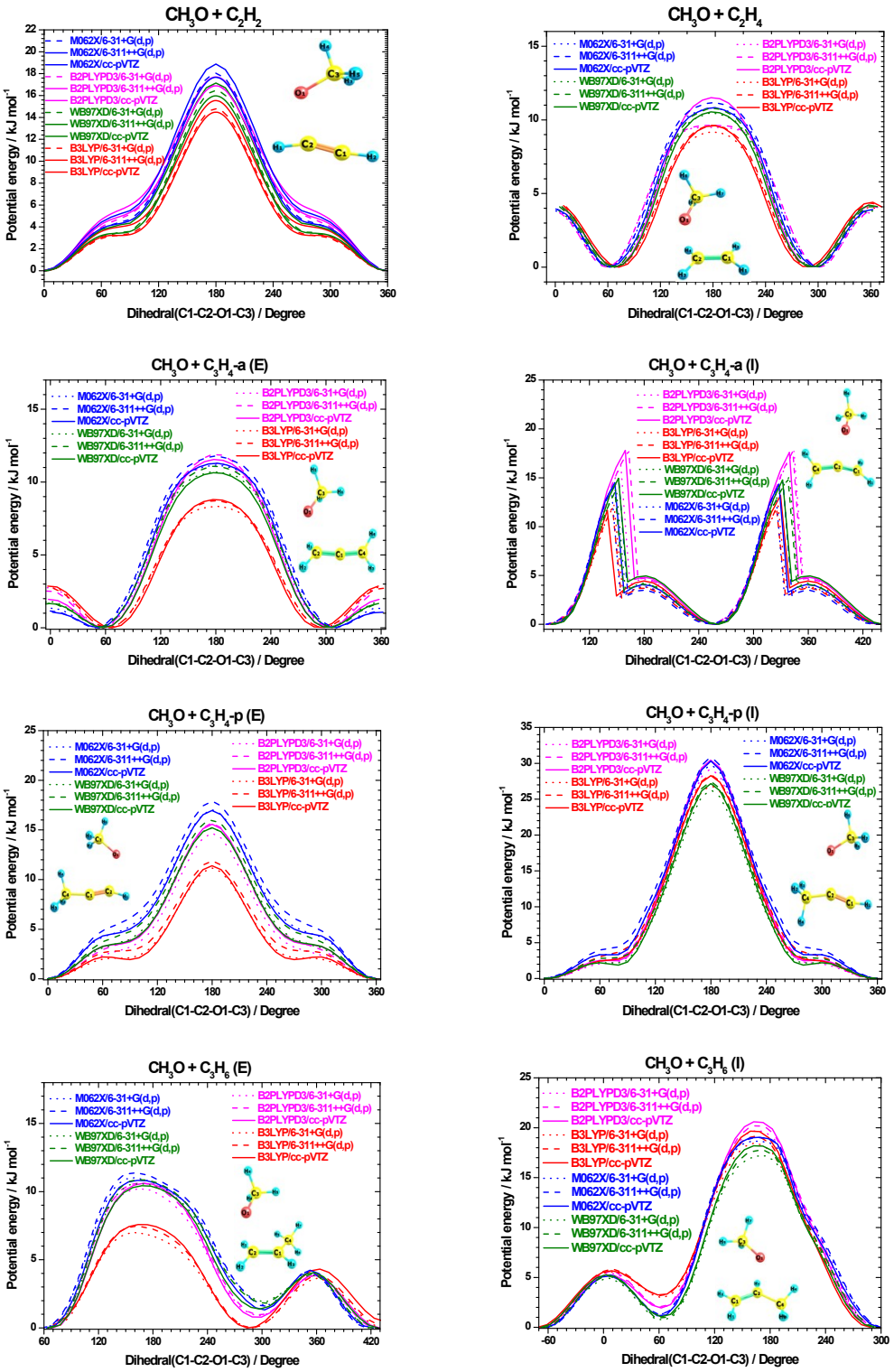

Fig. S8 Hindrance potentials for the newly formed methyl rotors of $CH_3\dot{O}$ radical additions to C_2H_2/C_2H_4/C_3H_4-a/C_3H_4-p/C_3H_6 calculated at twelve DFT methods.

9. The relative energy deviations between DFT and DLPNO-CCSD(T)/CBS results for the newly formed rotors of $\dot{C}H_3/\dot{C}_2H_3/\dot{C}_2H_5/CH_3\dot{O}$ radical additions to C_2H_2/C_2H_4.

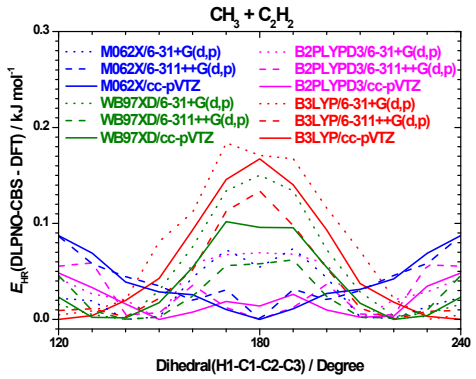

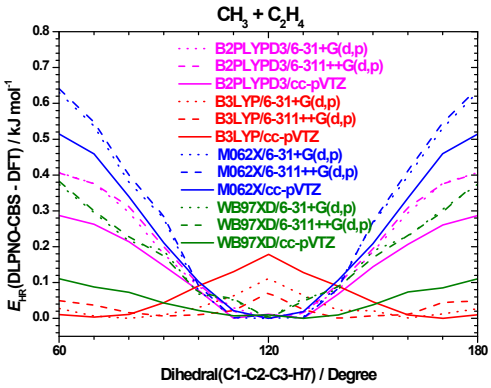

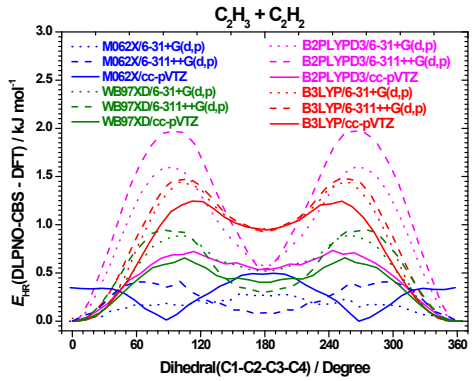

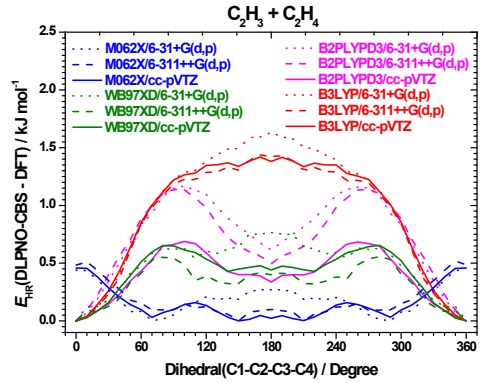

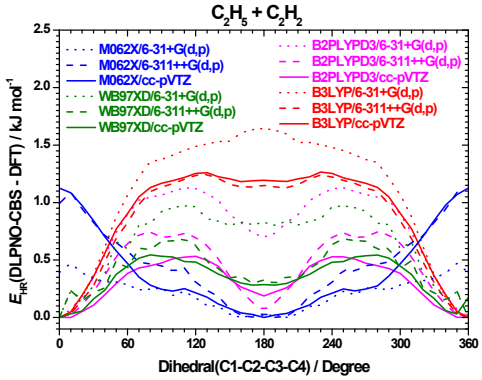

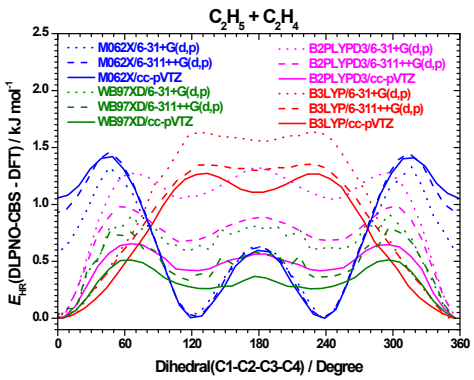

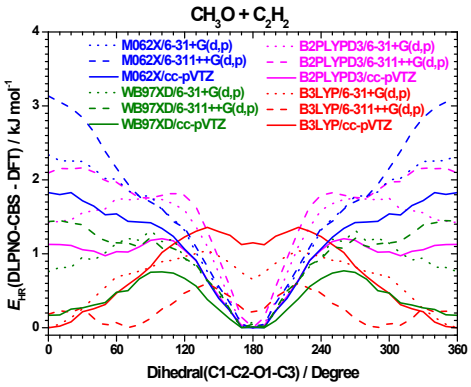

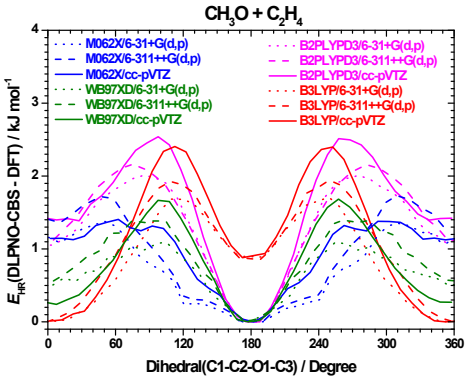

Fig. S9 The relative potential energy differences calculated by DFT and DLPNO-CCSD(T)/CBS methods for rotors formed by $\dot{C}H_3/\dot{C}_2H_3/\dot{C}_2H_5/CH_3\dot{O}$ radical additions to C_2H_2 and C_2H_4, and potential energy differences are relative to the lowest energy difference of each hindrance potential.

10. The percentage deviations between DFT and the corresponding mean energies for rotors formed by $\dot{C}H_3/\dot{C}_2H_3/\dot{C}_2H_5/CH_3\dot{O}$ radical additions to C_2H_2/C_2H_4 at 500 K, 1000 K and 2000 K.

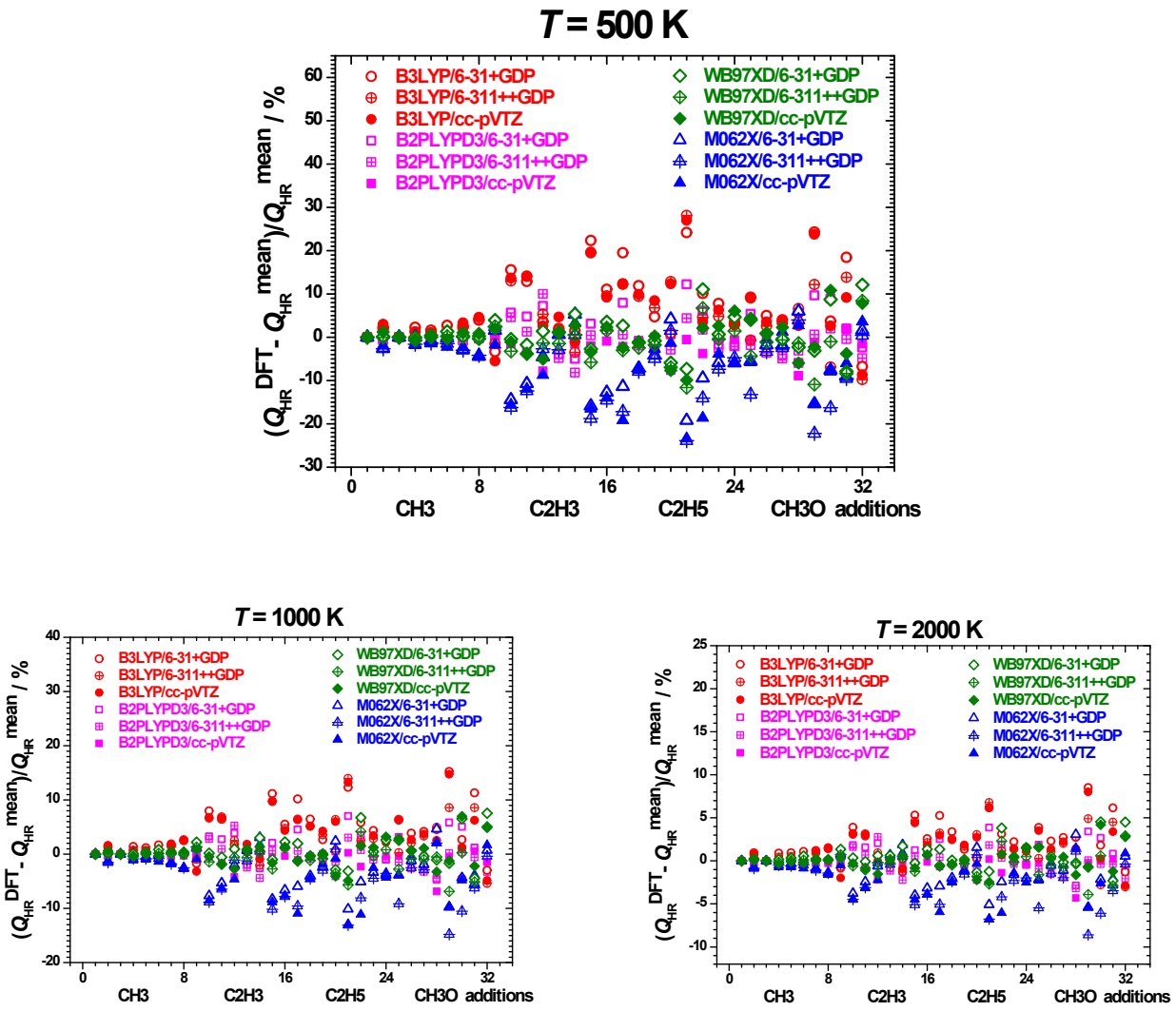

Fig. S10 The percentage deviations between DFT and the corresponding mean energies for rotors formed by $\dot{C}H_3/\dot{C}_2H_3/\dot{C}_2H_5/CH_3\dot{O}$ radical additions to C_2H_2/C_2H_4 at 500 K, 1000 K and 2000 K.

11. The maximum E_{HR}(DLPNO-CCSD(T)/CBS – DFT) for rotors formed through $\dot{C}H_3/\dot{C}_2H_3/\dot{C}_2H_5/CH_3\dot{O}$ radical additions to C_2H_2/C_2H_4.

Table S7 The maximum deviations of hindrance potential energies between DFT and DLPNO-CCSD(T) methods for rotors formed through $\dot{C}H_3/\dot{C}_2H_3/\dot{C}_2H_5/CH_3\dot{O}$ radical additions to C_2H_2/C_2H_4.

ΔE_{HR}(MAX)	B2PLYP-D3			B3LYP			M06-2X			ωB97X-D		
	6-31+G(d,p)	6-311++G(d,p)	cc-pVTZ	6-31+G(d,p)	6-311++G(d,p)	cc-pVTZ	6-31+G(d,p)	6-311++G(d,p)	cc-pVTZ	6-31+G(d,p)	6-311++G(d,p)	cc-pVTZ
TS1	0.07	0.06	0.05	0.18	0.13	0.17	0.07	0.09	0.09	0.15	0.06	0.10
TS2	0.41	0.41	0.29	0.11	0.07	0.18	0.63	0.64	0.51	0.37	0.38	0.11
TS9	1.60	1.97	0.73	1.44	1.48	1.25	0.29	0.42	0.50	0.88	0.95	0.66
TS10	1.17	1.14	0.69	1.63	1.44	1.42	0.44	0.52	0.46	0.76	0.56	0.65
TS17	1.13	0.74	0.53	1.64	1.24	1.27	0.47	1.09	1.13	0.97	0.68	0.54
TS18	1.33	0.99	0.65	1.64	1.35	1.27	1.33	1.46	1.42	0.92	0.80	0.51
TS25	1.75	2.16	1.20	1.04	0.60	1.36	2.34	3.13	1.83	1.32	1.45	0.77
TS26	2.01	2.16	2.54	1.71	1.94	2.41	1.38	1.73	1.41	1.10	1.39	1.68

12. The maximum deviations of hindered internal rotation partition function between DFT and DLPNO-CCSD(T) methods for rotors formed through $\dot{C}H_3/\dot{C}_2H_3/\dot{C}_2H_5/CH_3\dot{O}$ radical additions to C_2H_2/C_2H_4.

Table S8 The maximum deviations of Q_{HR} between DFT and DLPNO-CCSD(T) methods for rotors formed through $\dot{C}H_3/\dot{C}_2H_3/\dot{C}_2H_5/CH_3\dot{O}$ radical additions to C_2H_2/C_2H_4.

ΔQ_{HR}(MAX)	B2PLYP-D3			B3LYP			M06-2X			ωB97X-D		
	6-31+G(d,p)	6-311++G(d,p)	cc-pVTZ	6-31+G(d,p)	6-311++G(d,p)	cc-pVTZ	6-31+G(d,p)	6-311++G(d,p)	cc-pVTZ	6-31+G(d,p)	6-311++G(d,p)	cc-pVTZ
TS1	0.25	-0.28	1.11	0.68	0.35	-0.40	0.89	0.28	-0.18	0.98	-0.50	0.59
TS2	-4.17	-4.10	-2.87	0.44	-0.31	1.38	-6.30	-6.42	-5.19	-3.29	-3.37	-1.08
TS9	-4.58	-6.47	-4.10	-5.80	-4.79	-9.05	-3.88	-0.13	-6.88	-0.61	-1.15	-1.79
TS10	23.38	21.55	11.74	36.79	32.43	33.71	-6.76	-8.48	-8.25	12.85	8.47	12.58
TS17	9.57	30.78	-16.55	9.94	24.52	13.61	40.57	29.52	-5.82	-14.23	17.16	8.60
TS18	-5.19	-6.22	-4.21	13.08	8.82	9.67	-13.18	-13.95	-13.15	-5.14	-6.83	-4.41
TS25	4.69	-3.34	-1.44	13.06	-0.97	12.12	-6.51	-14.90	-5.69	6.05	-4.71	6.39
TS26	-5.45	-7.26	-4.36	0.37	-2.25	-1.33	-4.82	-5.79	-3.36	-2.13	-4.47	-2.49